Archives of Biochemistry and Biophysics 480 (2008) 75–84

Contents lists available at ScienceDirect

Archives of Biochemistry and Biophysics

journal homepage: www.elsevier.com/locate/yabbi

Evidence that the bZIP domains of the Jun transcription factor bind to DNA as monomers prior to folding and homodimerization

Kenneth L. Seldeen, Caleb B. McDonald, Brian J. Deegan, Amjad Farooq *

Department of Biochemistry & Molecular Biology and the UM/Sylvester Braman Family Breast Cancer Institute, Leonard Miller School of Medicine, University of Miami, Miami, FL 33136, United States

ARTICLE INFO

Article history:
Received 15 September 2008
and in revised form 6 October 2008
Available online 12 October 2008

Keywords:
Protein–DNA thermodynamics
Isothermal titration calorimetry
Jun Transcription factor
Basic leucine zipper bZIP
DNA promoter elements TRE and CRE

ABSTRACT

The Jun oncoprotein belongs to the AP1 family of transcription factors that is collectively engaged in diverse cellular processes by virtue of their ability to bind to the promoters of a wide spectrum of genes in a DNA sequence-dependent manner. Here, using isothermal titration calorimetry, we report detailed thermodynamics of the binding of bZIP domain of Jun to synthetic dsDNA oligos containing the TRE and CRE consensus promoter elements. Our data suggest that binding of Jun to both sites occurs with indistinguishable affinities but with distinct thermodynamic signatures comprised of favorable enthalpic contributions accompanied by entropic penalty at physiological temperatures. Furthermore, anomalously large negative heat capacity changes observed provoke a model in which Jun loads onto DNA as unfolded monomers coupled with subsequent folding and homodimerization upon association. Taken together, our data provide novel insights into the energetics of a key protein–DNA interaction pertinent to cellular signaling and cancer. Our study underscores the notion that the folding and dimerization of transcription factors upon association with DNA may be a more general mechanism employed in protein–DNA interactions and that the conventional school of thought may need to be re-evaluated.

Introduction

The Jun oncoprotein is a component of the transcription factor AP1 (activator protein 1)[1] that couples extracellular information in the form of growth factors, cytokines, hormones and stress to DNA transcription and, in so doing, orchestrates a diverse array of cellular processes such as cell growth and proliferation, cell cycle regulation, embryonic development and cancer. Jun unleashes its transcriptional activity by virtue of its ability to recognize the pseudo-palindromic TGACTCA and palindromic TGACGTCA consensus sequences found in the promoters of a multitude of genes such as metallothionein IIa, collagenase, interleukin 2 and cyclin D1 either as a homodimer or alternatively as a heterodimer in complex with a related oncoprotein Fos [1,2]. In recent years, new members of the AP1 family, such as ATF and Maf, that can also act as dimerization partners for Jun have been discovered [3,4]. The consensus sequences TGACT CA and TGACGTCA, respectively referred to as the TPA (12-*O*-tetradecanoylphorbol-13-acetate) response element (TRE) and the cAMP response element (CRE), occur with a high frequency in the human genome [5,6]. Jun is expressed in a wide variety of tissues and is subject to activation by a diverse array of mitogenic inputs, including up-regulation by MAP kinases [7,8]. Upon activation, Jun can switch on gene transcription via homodimerization or heterodimerization with one of the members of the AP1 family as well as through its co-operation with other transcription factors in the recruitment of the transcriptional machinery to the site of DNA [2,6,9–11]. However, the ability of Jun to heterodimerize with Fos not only changes its specificity but is also believed to substantially enhance its transcriptional activity as demonstrated through the transforming potential of the Jun-Fos heterodimer in a wide variety of mammalian cells [2,10,11].

The ability of Jun to recognize DNA sequences at the promoters of specific genes resides in a region that has come to be known as the basic zipper (bZIP) domain (Fig. 1a). The bZIP domain can be further dissected into two well-defined functional subdomains termed the basic region (BR) at the N-terminus followed by the leucine zipper (LZ) at the C-terminus. The leucine zipper is a highly conserved protein module found in a wide variety of transcription factors and structural proteins and contains a signature leucine at every seventh position within the five successive heptads of amino acid residues. The leucine zippers adapt continuous α-helical conformations and induce Jun-Jun homodimerization or its heterodimerization with other members of AP1 family by virtue of their ability to wrap around each other in a coiled coil dimer [12,13]. Such intermolecular arrangement brings the basic regions at the N-termini of bZIP domains into close proximity and thereby

* Corresponding author. Fax: +1 305 243 3955.
E-mail address: amjad@farooqlab.net (A. Farooq).

[1] *Abbreviations used:* AP1, activator protein 1; BR, basic region; His, polyhistidine tag; ITC, isothermal titration calorimetry; LZ, leucine zipper; MAP, mitogen-activated protein; SASA, solvent accesible surface area; Trx, thioredoxin; bZIP, basic zipper.

0003-9861/$ - see front matter © 2008 Elsevier Inc. All rights reserved.
doi:10.1016/j.abb.2008.10.010

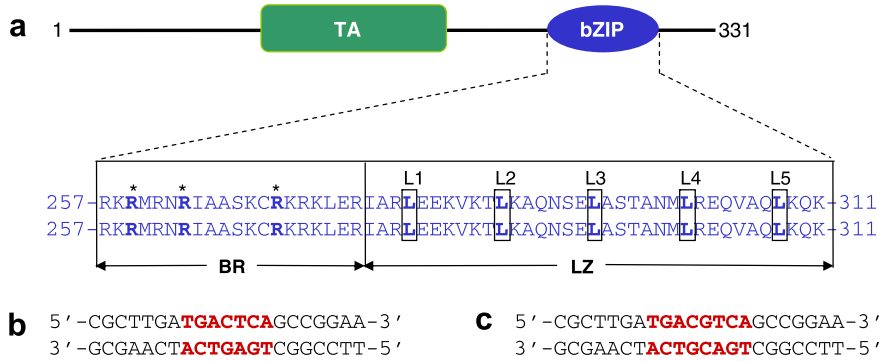

Fig. 1. Protein and DNA sequences. (a) A schematic showing domain organization of the transcription factor Jun. The basic zipper (bZIP) domain responsible for sequence-specific recognition of DNA at the promoter regions is located C-terminal to the transactivation (TA) domain. The amino acid sequence of the bZIP domain is shown in duplicate to illustrate how two monomers associate to generate a homodimer. The sequence boundaries of the N-terminal basic region (BR) and the C-terminal leucine zipper (LZ) subdomains are also demarcated. The five signature leucines (L1–L5) characteristic of LZ subdomains, spaced exactly six residues apart, are boxed and bold faced. The basic residues in the BR subdomains that contact the DNA bases and the backbone phosphates are indicated by asterisks and bold faced. (b) Nucleotide sequence of 21-mer dsDNA oligo containing the TRE site (bold faced and colored red). (c) Nucleotide sequence of 22-mer dsDNA oligo containing the CRE site (bold faced and colored red). (For interpretation of the references to color in this figure legend the reader is referred to the web version of the paper.)

enables them to insert into the major grooves of DNA at the promoter regions in an optimal fashion in a manner akin to a pair of forceps. While the α-helices are held together by numerous inter-helical hydrophobic contacts and salt bridges, hydrogen bonding between the sidechains of basic residues in the basic regions and the sidechains of nucleotides accounts for high affinity binding of bZIP domains to DNA [2,12,14]. It is widely believed that the basic regions within the bZIP domains are unstructured in the absence of DNA and undergo folding to adapt α-helical conformations only upon DNA binding [15]. This notion was further confirmed by our recent thermodynamic studies on the binding of Jun-Fos heterodimer to DNA, wherein we reasoned that the heat capacity changes accompanying this interaction could only be explained by the coupling of folding of basic regions upon association with DNA [16]. This previous study also demonstrated that the binding of DNA to Jun-Fos heterodimer is largely driven by favorable enthalpic changes accompanied by entropic penalty at physiological temperatures.

In an effort to further our understanding of the relationship between structure and thermodynamics governing the binding of the members of the AP1 family to DNA, we have employed isothermal titration calorimetry (ITC) to delineate the thermodynamics of the binding of the bZIP domain of Jun to synthetic dsDNA oligos containing the TRE and CRE consensus promoter elements. Our data suggest that binding of Jun to both sites occurs with indistinguishable affinities but with distinct thermodynamic signatures comprised of favorable enthalpic contributions accompanied by entropic penalty at physiological temperatures. Furthermore, anomalously large negative heat capacity changes observed provoke a model in which Jun loads onto DNA as unfolded monomers coupled with subsequent folding and homodimerization upon association. Taken together, our data provide novel insights into the energetics of a key protein–DNA interaction pertinent to cellular signaling and cancer. Our study underscores the notion that the folding and dimerization of transcription factors upon association with DNA may be a more general mechanism employed in protein–DNA interactions and that the conventional school of thought may need to be re-evaluated.

Materials and methods

Sample preparation

bZIP domain of human Jun (residues 251–331) was cloned into pET102 bacterial expression vector, with an N-terminal thioredoxin (Trx)-tag and a C-terminal polyhistidine (His)-tag, using Invitrogen TOPO technology. The recombinant protein was expressed, purified and characterized as described previously [16]. Total monomeric concentration of bZIP domain was determined by the fluorescence-based Quant-It assay (Invitrogen) and spectrophotometrically using an extinction co-efficient of 14,230 $M^{-1}cm^{-1}$ at 280 nm. The extinction co-efficient was calculated using the online software ProtParam at ExPasy Server [17]. Results from both methods were in an excellent agreement. HPLC-grade DNA oligos containing the consensus TRE and CRE sites were commercially obtained from Sigma Genosys. The complete nucleotide sequences of these oligos are presented in Fig. 1b and c. Oligo concentrations were determined spectrophotometrically on the basis of their extinction co-efficients derived from their nucleotide sequences using the online software OligoAnalyzer 3.0 (Integrated DNA Technologies) based on the nearest-neighbor model [18]. Double-stranded DNA (dsDNA) annealed oligos were generated as described previously [16].

ITC measurements

Isothermal titration calorimetry (ITC) experiments were performed on Microcal VP-ITC instrument and data were acquired and processed using fully automized features in Microcal ORIGIN software. All measurements were repeated two to three times. Briefly, the bZIP domain of Jun and dsDNA oligos were prepared in 50 mM Tris, 200 mM NaCl, 1 mM EDTA and 5 mM β-mercaptoethanol at pH 8.0. Because of its low stability as stated earlier [16], the bZIP domain of Jun was concentrated to about 10 μM using the Amicon Ultra-15 centrifugal filter units (MWCO 10 kD) immediately prior to running the experiments. All samples were de-gassed using the ThermoVac accessory for 10 min. The experiments were initiated by injecting 20 × 10 μl injections of 50–100 μM of dsDNA oligo from the syringe into the calorimetric cell containing 1.8 ml of 5–10 μM of the dimer-equivalent bZIP domain at a fixed temperature in the narrow range of 15–35 °C. The change in thermal power as a function of each injection was automatically recorded using Microcal ORIGIN software and the raw data were further processed to yield binding isotherms of heat release per injection as a function of DNA to protein molar ratio. The heats of mixing and dilution were subtracted from the heat of binding per injection by carrying out a control experiment in which the same buffer in the calorimetric cell was titrated against the dsDNA oligos in an identical manner. Control experiments with scrambled dsDNA oligos generated similar thermal power to that obtained for

the buffer alone – as did the titration of dsDNA oligos containing TRE and CRE sites against a protein construct containing thioredoxin with a C-terminal His-tag (Trx-His). Titration of concentrated Trx-His protein construct into the calorimetric cell containing the bZIP domain produced no observable signal, implying that neither Trx-tag nor His-tag interact with the bZIP domain of Jun. To extract the binding affinity (K_d) and the binding enthalpy (ΔH), the binding isotherms were iteratively fit to the following built-in function by non-linear least squares regression analysis using the integrated Microcal ORIGIN software:

$$q(i) = (n\Delta HVP/2)\{[1 + (L/nP) + (K_d/nP)] - [[1 + (L/nP) + (K_d/nP)]^2 - (4L/nP)]^{1/2}\} \quad (1)$$

where $q(i)$ is the heat release (kcal/mol) for the ith injection, n is the binding stoichiometry, V is the effective volume of protein solution in the calorimetric cell (1.46 ml), P is the total protein concentration in the calorimetric cell (μM) and L is the total concentration of DNA added (μM). Given that Jun monomers freely exchange with their dimeric counterparts at equilibrium, P was assumed to be equivalent to the total experimentally measured monomeric concentration of bZIP domain. It should be noted that the above equation is derived from the binding of a ligand to a macromolecule using the law of mass action [19].

SASA calculations

The magnitude of changes in polar and apolar solvent-accessible surface area (SASA) in the bZIP domain of Jun upon binding to dsDNA oligos containing the TRE and CRE consensus sites were calculated from thermodynamic data obtained using ITC and compared with those obtained from structural data based on the 3D structural models (see below).

For calculation of changes in polar SASA ($\Delta SASA_{polar}$) and apolar SASA ($\Delta SASA_{apolar}$) upon the binding of dsDNA oligos containing the TRE and CRE consensus sites to bZIP domain of Jun from thermodynamic data, it was assumed that ΔC_p and ΔH at 60 °C (ΔH_{60}) are additive and linearly depend on the change in $\Delta SASA_{polar}$ and $\Delta SASA_{apolar}$ as embodied in the following empirically-derived expressions [20–23]:

$$\Delta C_p = a[\Delta SASA_{polar}] + b[\Delta SASA_{apolar}] \quad (2)$$

$$\Delta H_{60} = c[\Delta SASA_{polar}] + d[\Delta SASA_{apolar}] \quad (3)$$

where a, b, c and d are empirically-determined co-efficients with values of −0.26 cal/mol/K/Å^2, +0.45 cal/mol/K/Å^2, +31.34 cal/mol/Å^2 and −8.44 cal/mol/Å^2, respectively. The co-efficients a and b are independent of temperature, while c and d are referenced against a temperature of 60 °C, which equates to the median melting temperature of the proteins from which these constants are derived [20–23]. ΔC_p was calculated from the slope of a plot of ΔH versus temperature in the narrow temperature range of 15–35 °C for the binding of TRE and CRE dsDNA oligos to the bZIP domain of Jun using the ITC instrument. ΔH_{60} was calculated by the extrapolation of a plot of ΔH versus temperature to 60 °C for the binding of TRE and CRE dsDNA oligos to the bZIP domain of Jun using the ITC instrument. With ΔC_p and ΔH_{60} experimentally determined using ITC and the knowledge of co-efficients a–d from empirical models [20,24–27], equations (2) and (3) were simultaneously solved to obtain the magnitude of changes in $\Delta SASA_{polar}$ and $\Delta SASA_{apolar}$ independent of structural information upon the binding of dsDNA oligos to the bZIP domain of Jun.

To determine changes in $\Delta SASA_{polar}$ and $\Delta SASA_{apolar}$ upon the binding of dsDNA oligos containing TRE and CRE sequences to bZIP domain of Jun from structural data, three models of binding were assumed – the Lock-and-Key (LK) model, the Induced Fit (IF) model and the Equilibrium Shift (ES) model. In the LK model, it was assumed that the bZIP domains exist as fully folded homodimers and undergo no conformational change upon DNA binding – that is the homodimers exist in a pre-formed conformation that best fits the DNA. In the IF model, it was assumed that the bZIP domains exist as partially folded homodimers in which the basic regions are fully unstructured and only become structured upon DNA binding – that is DNA binding induces the folding of basic regions within otherwise pre-formed homodimers. In the ES model, it was assumed that the fully folded and the partially folded bZIP homodimers exist in equilibrium with the fully unfolded bZIP monomers and that DNA only binds to the monomers resulting in their folding and homodimerization – that is the bZIP domains bind to DNA as unfolded monomers such that their folding and homodimerization in association with DNA shifts the equilibrium with fully folded and partially folded homodimers in their direction. Changes in $\Delta SASA_{polar}$ and $\Delta SASA_{apolar}$ upon the binding of dsDNA oligos to bZIP domain of Jun from structural data were calculated using the following relationships:

$$\Delta SASA_{polar} = SASA_{bp} - (SASA_{fp} + SASA_{dp}) \quad (4)$$

$$\Delta SASA_{apolar} = SASA_{ba} - (SASA_{fa} + SASA_{da}) \quad (5)$$

where $SASA_{bp}$ and $SASA_{ba}$ are the polar and apolar SASA of bZIP homodimers bound to DNA, $SASA_{fp}$ and $SASA_{fa}$ are the polar and apolar SASA of fully folded bZIP homodimers alone, or partially folded bZIP homodimers alone, or fully unfolded bZIP monomers alone, and $SASA_{dp}$ and $SASA_{da}$ are the polar and apolar SASA of dsDNA oligos alone. For all three above-mentioned models of binding, $SASA_{bp}$ and $SASA_{ba}$ were calculated from structural models of bZIP homodimer in complex with dsDNA oligos containing atomic coordinates of both the bZIP domains and the corresponding sense and antisense dsDNA oligos, while $SASA_{dp}$ and $SASA_{da}$ were calculated from the same structural models of bZIP homodimer in complex with dsDNA oligos but containing atomic coordinates of only the corresponding sense and antisense dsDNA oligos. For the LK model, $SASA_{fp}$ and $SASA_{fa}$ were calculated from structural models of bZIP homodimer in complex with dsDNA oligos but containing atomic coordinates of the bZIP domains only. For the IF model, $SASA_{fp}$ and $SASA_{fa}$ were calculated from structural models of bZIP homodimer determined in the absence of DNA with basic regions allowed to adopt unfolded conformations (see below). For the ES model, $SASA_{fp}$ and $SASA_{fa}$ were calculated from structural models of bZIP monomers with compact unfolded conformations. All SASA calculations were performed using the online software GETAREA with a probe radius of 1.4 Å [28].

Structural analysis

3D structures of bZIP domains of Jun as fully unfolded monomers alone, as partially folded homodimers alone and as fully folded homodimers bound to dsDNA oligos containing TRE and CRE sites were modeled using the MODELLER software based on homology modeling [29]. The model of bZIP domains of Jun-Jun homodimer in complex with 21-mer dsDNA oligo containing the TRE site was obtained using the crystal structure of bZIP domains of Jun-Jun homodimer in complex with a dsDNA oligo containing the TRE consensus sequence TGACTCA but differing in flanking sequences as a template (with a PDB code of 2H7H). The model of bZIP domains of Jun-Jun homodimer in complex with 22-mer dsDNA oligo containing the CRE site was obtained using the crystal structure of bZIP domains of Jun-Jun homodimer in complex with a dsDNA oligo containing the CRE consensus sequence TGACGTCA but differing in flanking sequences as a template (with a PDB code of 1JNM). The model of bZIP domains of Jun-Jun as a partially folded homodimer in the absence of DNA was obtained using the crystal structure of leucine zippers of Jun-Jun homodimer alone as a template (with a PDB code of 1JUN) and the residues in the

N-terminal basic regions were allowed to adopt an open compact conformation and allowed to reach the energy minima without any restraints. The models of bZIP domains of Jun as fully unfolded monomers were obtained without a template with all residues allowed to adopt an open compact conformation and allowed to reach the energy minima without any restraints. 3D structural models of bZIP domains of Jun-Fos heterodimer in complex with dsDNA oligos containing TRE and CRE sites were modeled as described previously [16]. In each case, a total of 100 structural models were calculated and the structure with the lowest energy, as judged by the MODELLER Objective Function, was selected for further energy minimization in MODELLER prior to analysis. The structures were rendered using RIBBONS [30]. All other calculations were performed on the lowest energy-minimized structural model.

Table 1
Experimentally determined thermodynamic parameters for the binding of bZIP domain of Jun to dsDNA oligos containing TRE and CRE consensus sequences obtained from ITC measurements at 25 °C and pH 8.0.

	K_d (μM)	ΔH (kcalmol^{-1})	$T\Delta S$ (kcalmol^{-1})	ΔG (kcalmol^{-1})
TRE	0.06 ± 0.01	−24.23 ± 0.17	−14.30 ± 0.17	−9.92 ± 0.01
CRE	0.07 ± 0.02	−29.73 ± 0.59	−19.98 ± 0.44	−9.74 ± 0.14

The values for the binding affinity (K_d) and the binding enthalpy (ΔH) were obtained from the fit of a function as given in expression [1], based on the binding of a ligand to a macromolecule using the law of mass action assuming a 1:1 binding stoichiometry [19], to the ITC isotherms shown in Fig. 2. Free energy of binding (ΔG) was calculated from the relationship $\Delta G = RT\ln K_d$, where R is the universal molar gas constant (1.99 cal/mol/K) and T is the absolute temperature in Kelvins. Entropic contribution ($T\Delta S$) to binding was calculated from the relationship $T\Delta S = \Delta H - \Delta G$. The binding stoichiometries to the fits agreed to within ±10%. Errors were calculated from two to three independent measurements. All errors are given to one standard deviation.

Results and discussion

Jun-Jun homodimer binds to TRE and CRE with indistinguishable affinities but with distinct thermodynamic signatures

In an attempt to unravel the thermodynamic mechanism of the binding of bZIP domains of Jun-Jun homodimer to dsDNA oligos containing the TRE and CRE sites, we employed the technique of ITC (Fig. 2). Comparison of the various thermodynamic parameters is presented in Table 1. Our data suggest that the bZIP domains of Jun-Jun homodimer bind to TRE and CRE sites with virtually indistinguishable affinities. The notion that protein–ligand interactions cannot be merely understood in terms of their binding affinities could not be more applicable to the system being scrutinized here. Indeed, decomposition of the apparent binding affinities of TRE and CRE to Jun-Jun homodimer into their corresponding enthalpic (ΔH) and entropic ($T\Delta S$) components suggests that while both interactions are under strong enthalpic control accompanied by entropic penalty, these underlying forces contribute non-equally but in an opposing manner to the overall free energy of binding. Thus, while the binding of CRE to Jun-Jun homodimer is enthalpically more favorable by about +6 kcal/mol relative to TRE, binding of the latter is accompanied by roughly an equal but opposing gain of entropy relative to CRE, resulting in no overall differences in the affinity of these two DNA promoter elements to Jun-Jun homodimer. Although various attempts have been made in the past to obtain binding constants on the basis of non-continuous and non-quanti-

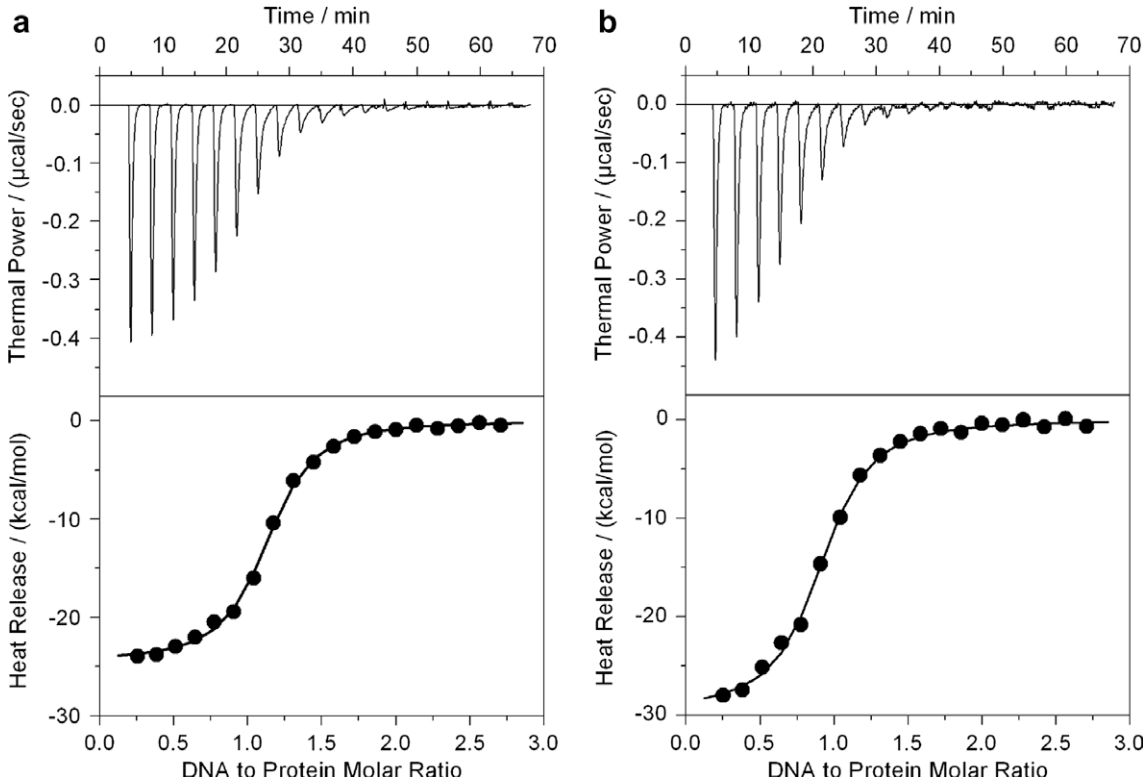

Fig. 2. ITC analysis of the binding of the bZIP domain of Jun to dsDNA oligos containing TRE (a) and CRE (b) consensus promoter sites. bZIP domain of Jun in the calorimetric cell was titrated with 25 × 10 μl injections of dsDNA oligo from the injection syringe at 25 °C and pH 8.0. The first injection and the corresponding heat release are not shown due to systematic uncertainties in the measurement. The top panels show the raw ITC data describing the change in thermal power as a function of time upon subsequent injections. The raw data were processed to generate the binding isotherms of heat release per injection as a function of increasing DNA to protein molar ratio as shown in the bottom panels. The solid lines represent the fit of the data in the binding isotherms to the function based on the binding of a ligand to a macromolecule using the Microcal ORIGIN software [19].

tative methods [13,31–34], this is the first study to not only report quantitative binding data but also detailed energetics governing the interaction of Jun-Jun homodimer to DNA.

What might be the molecular basis of favorable enthalpic change accompanied by entropic penalty for the interaction of TRE and CRE with Jun-Jun homodimer? The favorable enthalpic change is most likely due to the formation of hydrogen bonding, hydrophobic contacts and electrostatic interactions between the bZIP domains of Jun-Jun homodimer and its target DNA duplexes as observed in the 3D structure [14] – see also unpublished structures with PDB codes 1JNM and 2H7H. The more favorable enthalpic change of about +6 kcal/mol for the interaction CRE versus TRE to Jun-Jun homodimer may be attributed to the presence of an extra base pair between the TGA and TCA half-sites in CRE. It should be noted here that enthalpy-driven nature of protein–DNA interactions observed here is neither a rule nor an exception as numerous examples of protein–DNA interactions under enthalpic as well as entropic control have been reported previously [35–43]. Unlike the molecular basis for favorable enthalpic change, the rationale for the entropic penalty encountered here is less intuitive. It is widely believed that the net entropic change upon molecular associations largely results from interplay between two opposing entropic components – ΔS_{solv} and ΔS_{conf}. The ΔS_{solv} is the favorable entropy change due to enhancement in the degrees of freedom of solvent molecules as a result of their restructuring and displacement, particularly around apolar groups, upon molecular associations. In contrast, the ΔS_{conf} is the unfavorable entropic change that arises from the restriction of conformational degrees of freedom of the backbone and sidechain atoms upon molecular associations. It has been suggested that the basic regions in the bZIP domains are unstructured in the absence of DNA and undergo folding only upon DNA binding [15]. Thus, such restructuring of protein upon DNA binding could further negatively contribute to the ΔS_{conf}. Furthermore, it is believed that DNA also experiences some degree of bending and hence loss in conformational freedom upon binding to bZIP domains [44,45]. On the basis of the foregoing arguments, we attribute the unfavorable entropic change observed here upon the binding of bZIP domains of Jun-Jun homodimer to DNA largely to the loss of conformational degrees of freedom of backbone and sidechain atoms in both the protein and DNA as embodied in the term ΔS_{conf}. The less favorable entropic change of about −6 kcal/mol for the interaction of CRE versus TRE to Jun-Jun homodimer may be attributable to the presence of an extra base pair between the TGA and TCA half-sites in CRE.

Enthalpy and entropy compensate the effect of temperature on the binding of DNA to Jun-Jun homodimer

In an effort to determine the effect of temperature on the various thermodynamic parameters, we analyzed the binding of the bZIP domains of Jun-Jun homodimer to dsDNA oligos containing the TRE and CRE consensus sites in the temperature range of 15–35 °C (Fig. 3). Our data indicate that both the enthalpic (ΔH) and entropic ($T\Delta S$) contributions to the overall free energy of binding (ΔG) show strong temperature-dependence and that both ΔH and $T\Delta S$ largely compensate for each other to generate ΔG that is virtually independent of temperature. Thus, while ΔH and $T\Delta S$ experience more than 20 kcal/mol change in their contributions to binding in going from 15 °C to 35 °C, ΔG varies no more than 1 kcal/mol over the same temperature range. Consistent with this observation is the relatively constant nature of the binding affinity (0.05–0.15 μM) over the same temperature range for the interaction of both the TRE and CRE dsDNA oligos with the bZIP domains of Jun-Jun homodimer. The linear and opposing dependence of ΔH and $T\Delta S$ as a function of temperature, while maintaining a more or less constant ΔG, is a common feature observed in protein folding

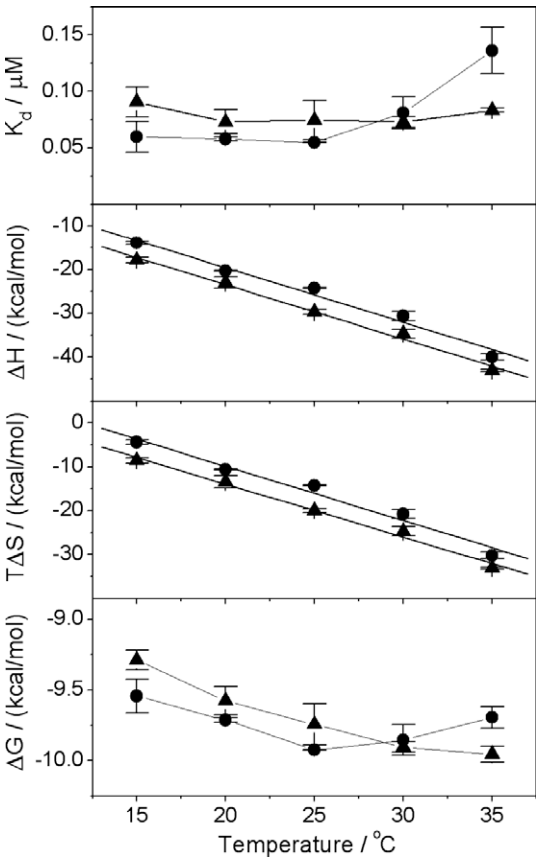

Fig. 3. Dependence of thermodynamic parameters K_d, ΔH, $T\Delta S$ and ΔG on temperature for the binding of bZIP domain of Jun to dsDNA oligos containing TRE (●) and CRE (▲) sites. bZIP domain of Jun in the calorimetric cell was titrated with 25 × 10 μl injections of dsDNA oligo from the injection syringe at various temperatures in the range of 15–35 °C at pH 8.0. To determine the various thermodynamic parameters, the binding isotherms were fit to the function based on the binding of a ligand to a macromolecule using the Microcal ORIGIN software [19]. Each data point is the arithmetic mean of two to three experiments. All error bars are given to one standard deviation. The solid lines for the ΔH and $T\Delta S$ plots show linear fits to the data, while the solid lines for the K_d and ΔG plots show straight lines connecting the data points for clarity.

and binding reactions [20,21,46]. This phenomenon gives rise to two key temperature points T_H and T_S – the temperatures where enthalpic (ΔH) and entropic ($T\Delta S$) contributions to the free energy of binding change sign, respectively. Thus, in the case of the binding of DNA to Jun-Jun homodimer, ΔH will become negative and hence thermodynamically favorable above T_H, while $T\Delta S$ will become negative and hence thermodynamically unfavorable above T_S. Table 2 provides the values for T_H and T_S accompanying the binding of DNA to the bZIP domains of Jun-Jun homodimer. As evidenced in Table 2, both T_H and T_S fall well below the physiological temperature of 37 °C, implying that the binding of Jun-Jun homodimer to DNA will be largely under enthalpic control accompanied by entropic penalty at physiological temperatures.

The temperature-dependence of ΔH is related to heat capacity of binding (ΔC_p) by Kirchhoff's relationship $\Delta C_p = d(\Delta H)/dT$. In other words, the slope of a plot of ΔH versus temperature equates to ΔC_p. Heat capacity is an important thermodynamic parameter in that it is related to the extent of the burial and dehydration of molecular surfaces from surrounding solvent molecules upon intermolecular association. This concept has come to be referred to as the change in solvent-accessible surface area (ΔSASA) [20,37,47,48]. In an attempt to understand how the binding of Jun-Jun homodimer to DNA affects SASA, we calculated ΔC_p values hovering around −1200 cal/mol/K from the slopes of ΔH versus

Table 2
Experimentally determined thermodynamic parameters for the binding of bZIP domain of Jun to dsDNA oligos containing TRE and CRE consensus sequences obtained from ITC measurements at various temperatures in the range of 15–35 °C and pH 8.0.

	T_H (°C)	T_S (°C)	ΔH_{60} (kcalmol^{-1})	ΔC_p (kcalmol^{-1}K^{-1})
TRE	−4.27 ± 0.28	+12.01 ± 0.01	−69.39 ± 1.71	−1.25 ± 0.04
CRE	−1.03 ± 1.50	+8.41 ± 1.16	−73.08 ± 1.82	−1.24 ± 0.06

The values for the various parameters shown were obtained as follows. The values for T_H, the temperature at which ΔH is zero, were obtained from the extrapolation of linear fits to the ΔH versus temperature plots (Fig. 3). The values for T_S, the temperature at which $T\Delta S$ is zero, were obtained from the extrapolation of linear fits to the $T\Delta S$ versus temperature plots (Fig. 3). The values for ΔH_{60}, the enthalpy at 60 °C, were obtained from the extrapolation of linear fits to the ΔH versus temperature plots (Fig. 3). The values for ΔC_p, the heat capacity change, were obtained from the slopes of linear fits to the ΔH versus temperature plots (Fig. 3). Errors were calculated from two to three independent measurements. All errors are given to one standard deviation.

temperature plots for the binding of bZIP domains of Jun-Jun homodimer to TRE and CRE sites (Fig. 3 and Table 2). What might be the significance of such large negative values of ΔC_p observed here? A positive value of ΔC_p implies that the occlusion of polar surfaces dominates the intermolecular association over apolar surfaces [20,49,50]. The fact that ΔC_p is accompanied by large negative changes suggests strongly that the binding of bZIP domains of Jun-Jun homodimer to DNA involves substantial burial of hydrophobic residues with little contributions from polar residues. It should be noted here that protein–ligand interactions typically result in the magnitude of ΔC_p of less than −1000 cal/mol/K, while values of ΔC_p in the range of −1000 to −2000 cal/mol/K are characteristic of proteins undergoing folding due to burial of a large number of apolar groups as a result of hydrophobic effect. Could the rather large negative values of ΔC_p observed here reflect the plausible scenario that folding and homodimerization of bZIP domains of Jun may be coupled to DNA binding?

Jun-Jun homodimer binds to DNA with higher affinity than Jun-Fos heterodimer but the latter harbors more favorable enthalpic change

Our thermodynamic data reported here for the binding of Jun-Jun homodimer to DNA are in sharp contrast to the thermodynamic data reported previously for the binding of Jun-Fos heterodimer to DNA [16]. While Jun-Jun homodimer is observed to bind to TRE and CRE sites with an affinity of between 0.06 and 0.07 μM here, the Jun-Fos heterodimer was observed to do so with an affinity of between 0.15 and 0.21 μM in the previous study [16]. The binding of Jun-Jun homodimer to DNA has been widely believed to be weaker than that of Jun-Fos heterodimer on the basis of non-continuous and non-quantitative measurements [2,13,31–34]. Our present study however suggests that this is not the case but, on the contrary, it is the Jun-Jun homodimer that binds to DNA with an affinity that is over twofold greater than that of Jun-Fos heterodimer. Comparison of the differential binding affinities of Jun-Jun homodimer versus the Jun-Fos heterodimer to their cognate DNA sequences only provides a glimpse of the complete contrast in the thermodynamic picture of these key protein–DNA interactions.

In Fig. 4a, we present the differential thermodynamic signatures for the binding of TRE and CRE to Jun-Jun homodimer relative to Jun-Fos heterodimer on the basis of the data presented here and those reported earlier [16]. In this plot, a positive value of ΔΔH implies that the enthalpy change is less favorable for the binding of DNA to Jun-Jun homodimer relative to Jun-Fos heterodimer, while a positive value of $T\Delta\Delta S$ is indicative of favorable gain of entropy for the binding of DNA to Jun-Jun homodimer relative to Jun-Fos heterodimer. Thus, as evidenced, the binding of Jun-Fos heterodimer to DNA is enthalpically more favorable by about +7 kcal/mol relative to Jun-Jun homodimer. However, this is slightly more than offset by a gain of about +8 kcal/mol of favorable entropic change for the binding of Jun-Jun homodimer to DNA relative to Jun-Fos heterodimer resulting in an overall enhanced binding of the former transcription factor. Assuming that the overall entropic change results from two major opposing entropic forces, namely ΔS_{solv} and ΔS_{conf}, we further decomposed the overall favorable entropic gain of about +8 kcal/mol for the binding of Jun-Jun homodimer to DNA relative to Jun-Fos heterodimer into its constituent components to generate a plot of differential entropic signatures (Fig. 4b). In this plot, a positive value of ΔΔS implies that the entropy is more favorable for the binding of DNA to Jun-Jun homodimer relative to Jun-Fos heterodimer, a positive value of $\Delta\Delta S_{solv}$ indicates that the change in solvent entropy is more favorable for the binding of DNA to Jun-Jun homodimer relative to Jun-Fos heterodimer, and a negative value of $\Delta\Delta S_{conf}$ demonstrates that the change in conformational entropy harbors greater entropic penalty for the binding of DNA to Jun-Jun homodimer relative to Jun-Fos heterodimer. As shown, the binding of DNA to Jun-Jun homodimer leads to a favorable change in the solvent entropy of about 100 cal/mol/K but this is largely offset by a negative contribution to change in the conformational entropy of about −75 cal/mol/K. That this is so suggests strongly that the binding of the Jun-Jun homodimer to DNA is accompanied by a large conformational change in the

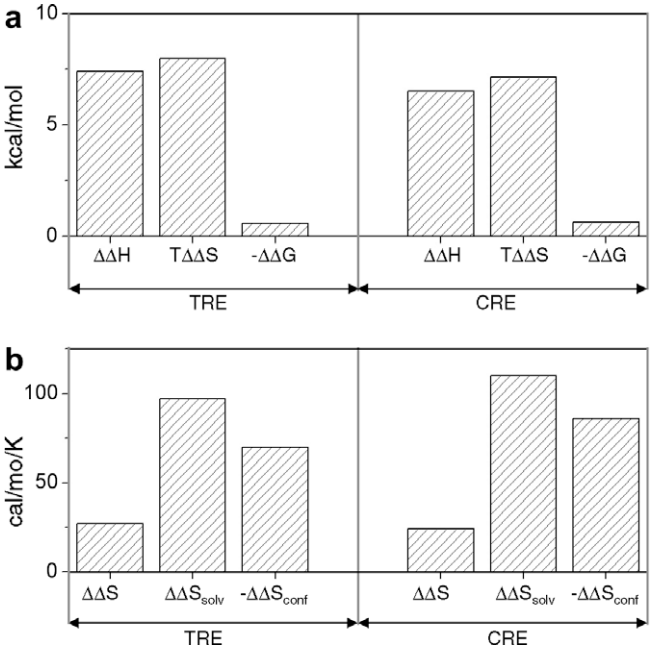

Fig. 4. Differential energetics for the binding of TRE and CRE dsDNA oligos to Jun-Jun homodimer versus Jun-Fos heterodimer. (a) Differential thermodynamic signatures for the binding of DNA to Jun-Jun homodimer relative to Jun-Fos heterodimer. $\Delta\Delta H$, $T\Delta\Delta S$ and $\Delta\Delta G$ were calculated from the relationships $\Delta\Delta H = \Delta H_{jj} - \Delta H_{jf}$, $T\Delta\Delta S = T\Delta S_{jj} - T\Delta S_{jf}$ and $\Delta\Delta G = \Delta G_{jj} - \Delta G_{jf}$, where the subscripts jj and jf denote the corresponding thermodynamic parameters for the binding of DNA to Jun-Jun homodimer and Jun-Fos heterodimer, respectively. (b) Differential entropic signatures for the binding of DNA to Jun-Jun homodimer relative to Jun-Fos heterodimer. $\Delta\Delta S$, $\Delta\Delta S_{solv}$ and $\Delta\Delta S_{conf}$ were calculated from the relationships $\Delta\Delta S = \Delta S_{jj} - \Delta S_{jf}$, $\Delta\Delta S_{solv} = \Delta S_{solv(jj)} - \Delta S_{solv(jf)}$ and $\Delta\Delta S_{conf} = \Delta S_{conf(jj)} - \Delta S_{conf(jf)}$, where the subscripts jj and jf denote the corresponding thermodynamic parameters for the binding of DNA to Jun-Jun homodimer and Jun-Fos heterodimer, respectively. ΔS_{solv} was calculated from the relationship $\Delta S_{solv} = \Delta C_p \ln[298/385]$ and ΔS_{conf} from the relationship $\Delta S_{conf} = \Delta S - \Delta S_{solv}$ for the binding of DNA to Jun-Jun homodimer or Jun-Fos heterodimer with the ΔS and ΔC_p being the corresponding thermodynamic parameters. Thermodynamic parameters for the binding of DNA to Jun-Jun homodimer are reported here, while those for the binding of DNA to Jun-Fos heterodimer were reported in the earlier study [16].

protein relative to Jun-Fos heterodimer. We will elaborate on the molecular nature of this conformational change in the latter part of this study but, for now, we turn our attention to delineating the molecular basis of the more favorable enthalpic change of about +7 kcal/mol observed here for the binding of DNA to Jun-Fos heterodimer relative to Jun-Jun homodimer (Fig. 4a).

Given that the enthalpic change largely results from the formation of hydrogen bonding, hydrophobic contacts and electrostatic interactions between molecular surfaces, we reasoned that the enthalpically more favorable binding of DNA to the Jun-Fos heterodimer relative to Jun-Jun homodimer may be a manifestation of the differential burial of nucleotides against the amino acid residues in the basic regions of Jun-Fos heterodimer versus the Jun-Jun homodimer due to the variation in the amino acid sequence of the two transcription factors. In Fig. 5, we present the differential burial of the nucleotides corresponding to the consensus sequences TGACTCA and TGACGTCA for TRE and CRE, respectively, upon the binding of DNA to Jun-Jun homodimer relative to Jun-Fos heterdimer. In these plots, a positive value of ΔSASA for a given nucleotide implies that it is buried more in association with Jun-Fos heterodimer relative to Jun-Jun homodimer, while a negative value of ΔSASA for a given nucleotide is indicative of greater burial in association with Jun-Jun homodimer relative to Jun-Fos heterodimer. Thus, for example, adenosine in the TGA half-site within the TRE sense strand buries more surface area in contact with Jun-Jun homodimer relative to Jun-Fos heterodimer, while cytidine in the TCA half-site within the TRE sense strand buries more surface area in contact with Jun-Fos heterodimer relative to Jun-Jun homodimer. Further differences in the extent to which nucleotides are buried upon interaction with Jun-Jun homodimer versus the Jun-Fos heterodimer can be found throughout the consensus sites of TRE and CRE. In short, the differential enthalpic changes observed upon the binding of DNA to Jun-Jun homodimer relative to Jun-Fos heterodimer may be attributable to the differential burial of nucleotides and amino acid residues upon their association.

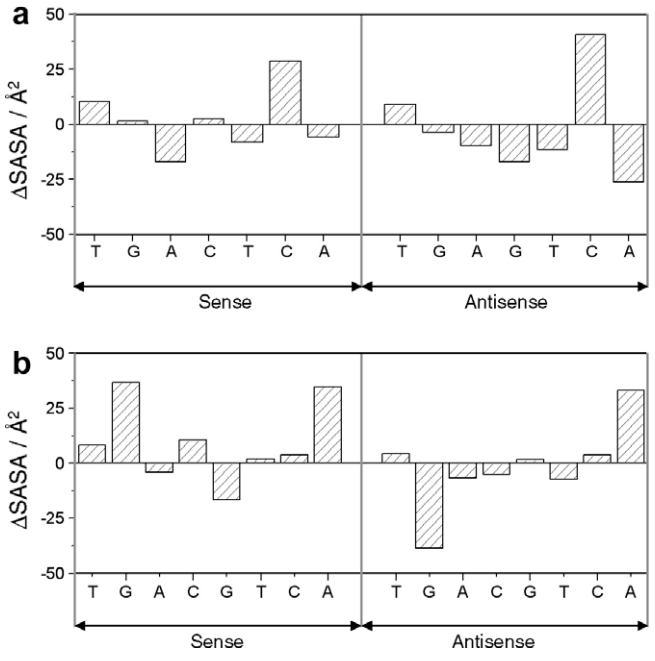

Fig. 5. Differential changes in SASA for the binding of TRE and CRE dsDNA oligos to Jun-Jun homodimer versus Jun-Fos heterodimer. (a) Differential changes in SASA observed for each nucleotide in the sense and antisense strands of TRE consensus site TGACTCA. ΔSASA for each nucleotide was calculated using the relationship $\Delta SASA = SASA_{jj} - SASA_{jf}$, where the subscripts jj and jf denote the SASA observed for each nucleotide for the binding of TRE to the bZIP domains of Jun-Jun homodimer and Jun-Fos heterodimer, respectively. (b) Differential changes in SASA observed for each nucleotide in the sense and antisense strands of CRE consensus site TGACGTCA. ΔSASA for each nucleotide was calculated using the relationship $\Delta SASA = SASA_{jj} - SASA_{jf}$, where the subscripts jj and jf denote the SASA observed for each nucleotide for the binding of CRE to the bZIP domains of Jun-Jun homodimer and Jun-Fos heterodimer, respectively.

Jun binds to DNA as a monomer with coupled folding and homodimerization of bZIP domains upon association

Experimental determination of values of ΔC_p combined with ΔH_{60} (enthalpy change at 60 °C) have been widely used to quantitatively calculate changes in polar SASA ($\Delta SASA_{polar}$), apolar SASA ($\Delta SASA_{apolar}$) and total SASA ($\Delta SASA_{total}$) upon intermolecular association [20,24–27] (Table 2). Such changes in SASA upon the binding of bZIP domains of Jun-Jun homodimer to DNA from our thermodynamic measurements are reported in Table 3. To rationalize what these numbers mean in terms of the mechanism of the protein–DNA interaction under scrutiny here, we also determined changes in SASA upon the binding of the bZIP domains of Jun to DNA from structural data independent of our thermodynamic measurements. To calculate such changes in SASA from structural data, we assumed three models of binding – the Lock-and-Key (LK) model, the Induced Fit (IF) model and the Equilibrium Shift (ES) model (Fig. 6). In the LK model, it was assumed that the bZIP domains exist as fully folded homodimers and undergo no conformational change upon DNA binding – that is the homodimers exist in a pre-formed conformation that best fits the DNA. Being the simplest and the classical model of protein–ligand interactions, the logic for the consideration of LK model needs no further light. In the IF model, it was assumed that the bZIP domains exist as partially folded homodimers in which the basic regions are fully unstructured and only become structured upon DNA binding – that is DNA binding induces the folding of basic regions within otherwise pre-formed homodimers. The justification for the IF model arises from the salient observation that the basic regions in bZIP domains are largely unstructured in the absence of DNA and undergo folding only upon binding to DNA [15,51–55]. In the ES model, it was assumed that the fully folded and the partially folded bZIP homodimers exist in equilibrium with the fully unfolded bZIP monomers and that DNA only binds to the monomers resulting in their folding and homodimerization – that is the bZIP domains bind to DNA as unfolded monomers such that their folding and homodimerization in association with DNA shifts the equilibrium with fully folded and partially folded homodimers in their direction. The ES model conjures support from the kinetic observation that the rate of dimerization of bZIP domains is significantly enhanced in the presence of DNA, implying that the bZIP domains associate with DNA as monomers coupled with their subsequent folding and dimerization [56]. The necessity for the fully unfolded monomers to be in equilibrium with the fully folded and the partially folded bZIP homodimers, as conjectured in the ES model, is due to the knowledge that the bZIP homodimers of Jun dissociate into monomers with a dissociation constant in the low micromolar range [57–59]. In light of this fact, it is thus logical to assume that the bZIP homodimers of Jun are likely to exist in equilibrium with monomers at the micromolar protein concentrations used in the calorimetric measurements recorded here. It is also of worthy note that the various states of Jun encompassing the fully unfolded and partially folded homodimer do not correspond to distinct conformations but rather should be considered as being comprised of an ensemble of conformations in agreement with previous studies [60,61].

Table 3 summarizes and compares values for $\Delta SASA_{polar}$, $\Delta SASA_{apolar}$ and $\Delta SASA_{total}$ upon the interaction of the bZIP domains of Jun to TRE and CRE sites from our thermodynamic and structural data. Our analysis shows that there are significant con-

Table 3
Changes in polar SASA ($\Delta SASA_{polar}$), apolar SASA ($\Delta SASA_{apolar}$) and total SASA ($\Delta SASA_{total}$) upon the binding of bZIP domain of Jun to dsDNA oligos containing TRE and CRE sites obtained from thermodynamic and structural data.

DNA site →	TRE				CRE			
Method →	Thermodynamic	Structural			Thermodynamic	Structural		
Model →	MI	LK	IF	ES	MI	LK	IF	ES
$\Delta SASA_{polar}$ (Å^2)	−3508	−1385	−2201	−3404	−3640	−1157	−1835	−3038
$\Delta SASA_{apolar}$ (Å^2)	−4805	−1343	−2168	−4701	−4859	−1360	−2453	−4986
$\Delta SASA_{total}$ (Å^2)	−8313	−2728	−4369	−8105	−8499	−2517	−4288	−8024

ΔSASA values based on thermodynamic data were obtained from the measurement of ΔC_p and ΔH_{60} for the binding of the bZIP domain of Jun to dsDNA oligos containing TRE and CRE sites (Fig. 3 and Table 2) using expressions (2) and (3), while ΔSASA values based on structural data were derived from 3D structural models of the bZIP domains of Jun alone and in complex with dsDNA oligos containing TRE and CRE sites (Fig. 6) using expressions (4) and (5). For ΔSASA values calculated from structural data, three models of binding were assumed – the Lock-and-Key (LK) model, the Induced Fit (IF) model and the Equilibrium Shift (ES) model (Fig. 6). In the LK model, it was assumed that the bZIP domains exist as fully folded homodimers and undergo no conformational change upon DNA binding – that is the homodimers exist in a pre-formed conformation that best fits the DNA. In the IF model, it was assumed that the bZIP domains exist as partially folded homodimers in which the basic regions are fully unstructured and only become structured upon DNA binding – that is DNA binding induces the folding of basic regions within otherwise pre-formed homodimers. In the ES model, it was assumed that the fully folded and the partially folded bZIP homodimers exist in equilibrium with the fully unfolded bZIP monomers and that DNA only binds to the monomers resulting in their folding and homodimerization – that is the bZIP domains bind to DNA as unfolded monomers such that their folding and homodimerization in association with DNA shifts the equilibrium with fully folded and partially folded homodimers in their direction. ΔSASA values calculated from thermodynamic data make no assumptions and are thus model-independent (MI).

flicts between the ΔSASA values calculated from thermodynamic data versus the LK and IF models of binding described above. In contrast, the values determined from thermodynamic data agree par excellence with those calculated from the ES model. While ΔSASA values determined from thermodynamic data are between two- and threefold greater than those determined from structural data assuming the LK and IF models, these values agree within about 5–10% to those calculated from structural data assuming the ES model. The small anomalies in ΔSASA values between those obtained from thermodynamic data versus those calculated from ES model are likely due to errors in the atomic coordinates of the structural models. On the same token, the semi-empirical expressions [2] and [3] used to calculate ΔSASA values from thermodynamic data are by no means ideal and their poor parametrization may have also contributed to the small anomalies observed here between ΔSASA values obtained from thermodynamic data versus those calculated from the ES model of protein–DNA interaction. An alternative explanation for such anomalies may also be due to the assumption that DNA experiences no conformational change upon interaction with the protein in spite of the evidence that it undergoes bending upon binding [44,45,62,63]. Nonetheless, this latter assumption is an excellent approximation in our a priori calculations of ΔSASA from structural data due to negligible occlusion of molecular surface in DNA upon bending compared to rather large surface area buried upon protein–DNA contacts coupled with protein folding. It is thus not surprising that, despite small anomalies, the ΔSASA values observed upon protein–DNA interaction calculated from thermodynamic data versus those calculated from the ES model show remarkable consistencies. In sum, our heat capacity measurements reported here strongly support a model whereby the bZIP domains of Jun load onto DNA as monomers such that association with DNA triggers their folding and homodimerization. That is to say that the DNA binding is coupled to the folding and homodimerization of bZIP domains of Jun.

Conclusions

Despite the knowledge of the significance of protein–DNA interactions to life for more than half a century, our understanding of the transient sequence of events leading up to the recognition of DNA by its protein counterparts hitherto remains abysmal. The classical picture based upon the notion of two rigid bodies coming together continues to strike a chord with most scientific literature and textbooks dealing with protein–DNA interactions. That this is so underlies the difficulties associated with unraveling the precise pathways by which transcription factors recognize specific response elements within the promoters of genes.

In an attempt to further our understanding of the mechanisms of protein–DNA interactions, we have reported herein thermodynamics of the binding of bZIP domains of the transcription factor Jun to its cognate TRE and CRE sites within DNA. Our study shows that while both TRE and CRE bind to bZIP domains with virtually indistinguishable affinities, the nature of underlying thermodynamic forces is quite different. Furthermore, in comparison with our previous study [16], the Jun-Jun homodimer binds to DNA with an affinity that is over twofold greater than that observed for the binding of Jun-Fos heterodimer. This key finding is in stark contrast to a number of previous studies whereby the binding of Jun-Fos heterodimer to DNA has been suggested to be stronger than that of Jun-Jun homodimer and epitomizes the power of ITC as a quantitative tool for the analysis of protein–DNA interactions [2,13,31–34]. The conventional view that the Jun-Fos heterodimer bound to DNA much stronger than Jun-Jun homodimer was in part resurrected due to the observation that the latter is a much weaker dimer than the former and that such differential dimer stability may be directly correlated with their binding potential [57–59]. On the contrary, the decreased stability of dimeric transcription factors may be a recipe for their enhanced binding potential to DNA through pathways that are kinetically more favorable as we have exquisitely shown here. It is also widely believed that the Jun-Fos heterodimer is a more potent activator of mitogenic transcription than the Jun-Jun homodimer and that such differential potency is largely due to the higher DNA-binding affinity of Jun-Fos heterodimer relative to Jun-Jun homodimer [2,13,31–34]. Our data presented here refute this long-held claim and suggest that differential transcriptional activities may be attributable to differential energetics in lieu of differential binding affinities. In light of this view, understanding the spatial and temporal specificity of transcription factors may require complete understanding of the underlying thermodynamic forces rather than mere analysis of their relative binding affinities.

Our heat capacity changes accompanying the Jun-DNA interaction are best accounted for by a model in which Jun monomers load onto DNA as monomers such that association with DNA triggers their folding and homodimerization. Because this model does not necessitate the requirement of a pre-formed Jun-Jun homodimer that best fits the DNA and given that Jun may largely exist as a monomer under physiological conditions due to its relatively

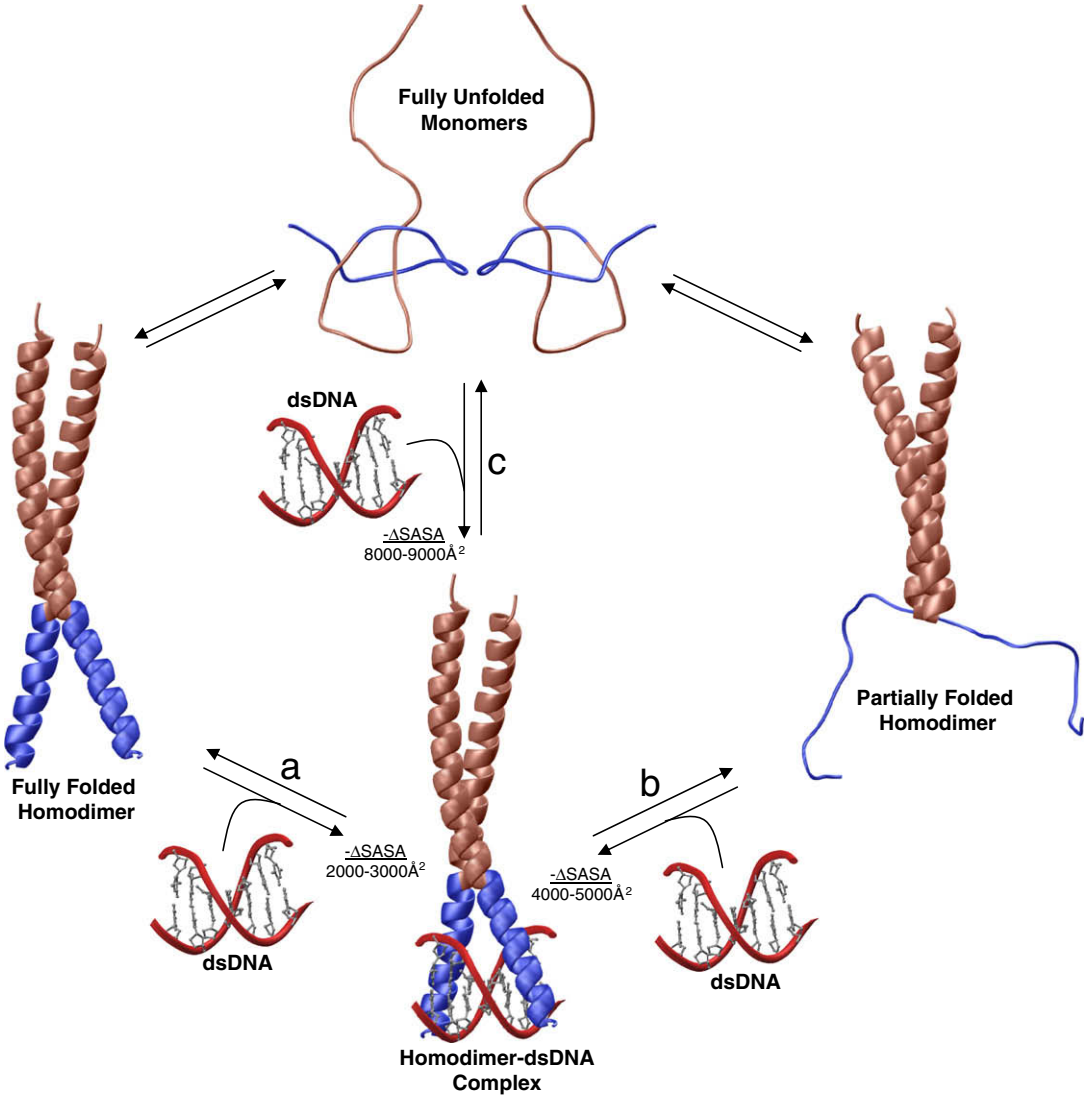

Fig. 6. Plausible pathways for the binding of bZIP domain of Jun to dsDNA oligo containing the consensus sequence TGACTCA via Lock-and-Key (LK), Induced Fit (IF) and Equilibrium Shift (ES) models. (a) In the LK model, the bZIP domains are envisaged to exist as fully folded homodimers and undergo no conformational change upon DNA binding – that is the homodimers exist in a pre-formed conformation that best fits the DNA. The LK model is expected to result in the total burial of SASA of between 2000 and 3000 Å^2. (b) In the IF model, the bZIP domains are presumed to exist as partially folded homodimers in which the basic regions are fully unstructured and only become structured upon DNA binding – that is DNA binding induces the folding of basic regions within otherwise pre-formed homodimers. The IF model is expected to result in the total burial of SASA of between 4000 and 5000 Å^2. (c) In the ES model, the fully folded and the partially folded bZIP homodimers are hypothesized to exist in equilibrium with the fully unfolded bZIP monomers but DNA only binds to the monomers resulting in their folding and homodimerization – that is the bZIP domains bind to DNA as unfolded monomers such that their folding and homodimerization in association with DNA shifts the equilibrium with fully folded and partially folded homodimers in their direction. The ES model is expected to result in the total burial of SASA of between 8000 and 9000 Å^2. 3D structures of bZIP domains alone and in complex with dsDNA oligo containing the TRE and CRE consensus sequences were determined using the MODELLER software. The dsDNA oligo shown contains the TRE consensus sequence TGACTCA with the DNA phosphate backbone depicted in red, while the sidechains of nucleotide bases are colored gray. For the bZIP domains shown, the leucine zippers are colored brown and the basic regions are in blue. (For interpretation of the references to color in this figure legend the reader is referred to the web version of the paper.)

weak dimer dissociation constant in the low micromolar range [57–59], it may also be the most favorable pathway under physiological conditions. However, such a mechanism does not mutually exclude other models in which Jun may bind to DNA as a fully folded or partially folded homodimer and only direct kinetic analysis can provide information on the most preferred pathway under non-equilibrium conditions. Nonetheless, kinetic studies have revealed that the bZIP domains of Jun and Fos associate with DNA as monomers coupled with their subsequent folding and heterodimerization [56]. In these studies, the heterodimerization of bZIP domains of Jun and Fos was best described by a single slow kinetic phase in the absence of DNA on the basis of fluorescence resonance energy transfer (FRET) between the two protein molecules. However, a second fast kinetic phase was observed when such heterodimerization was analyzed in the presence of DNA. Because no FRET was observed upon the interaction of pre-formed heterodimers with DNA, it was argued that the second fast kinetic phase must arise from the heterodimerization of Jun and Fos on DNA. This observation was further corroborated by the dependence of both the rate constant and the amplitude of the second fast kinetic phase upon DNA concentration. It is clearly evident that direct kinetic analysis of the binding of Jun to DNA using the above-mentioned FRET is not possible. However, we are pursuing a number of alternative strategies to decipher the preferred kinetic pathway by which Jun binds to DNA.

In conclusion, our thermodynamic analysis of Jun-DNA interaction suggests that the binding of transcription factors to DNA as monomers coupled with their subsequent folding and dimerization

may be a more common mechanism employed in protein–DNA interactions and that the conventional school of thought may need to be re-evaluated. Our future studies will be directed toward obtaining further evidence in support of this model. Nevertheless, our present study promises to break new ground and provokes further research on elucidating the precise kinetic pathways by which protein–DNA interactions ensue.

Acknowledgments

This work was supported by funds from the National Institutes of Health (Grant# R01-GM083897), the American Heart Association (Grant# 0655087B) and the UM/Sylvester Braman Family Breast Cancer Institute to AF.

References

[1] W. Lee, P. Mitchell, R. Tjian, Cell 49 (1987) 741–752.
[2] P. Angel, M. Karin, Biochim. Biophys. Acta 1072 (1991) 129–157.
[3] H. van Dam, M. Castellazzi, Oncogene 20 (2001) 2453–2464.
[4] K. Kataoka, M. Noda, M. Nishizawa, Mol. Cell. Biol. 14 (1994) 700–712.
[5] H. Zhou, T. Zarubin, Z. Ji, Z. Min, W. Zhu, J.S. Downey, S. Lin, J. Han, DNA Res. 12 (2005) 139–150.
[6] Y. Chinenov, T.K. Kerppola, Oncogene 20 (2001) 2438–2452.
[7] A.J. Whitmarsh, R.J. Davis, J. Mol. Med. 74 (1996) 589–607.
[8] R. Pramanik, X. Qi, S. Borowicz, D. Choubey, R.M. Schultz, J. Han, G. Chen, J. Biol. Chem. 278 (2003) 4831–4839.
[9] A.D. Baxevanis, C.R. Vinson, Curr. Opin. Genet. Dev. 3 (1993) 278–285.
[10] G. Raivich, A. Behrens, Prog. Neurobiol. 78 (2006) 347–363.
[11] K. Milde-Langosch, Eur. J. Cancer. 41 (2005) 2449–2461.
[12] T. Curran, B.R. Franza Jr., Cell 55 (1988) 395–397.
[13] T.D. Halazonetis, K. Georgopoulos, M.E. Greenberg, P. Leder, Cell 55 (1988) 917–924.
[14] J.N. Glover, S.C. Harrison, Nature 373 (1995) 257–261.
[15] L. Patel, C. Abate, T. Curran, Nature 347 (1990) 572–575.
[16] K.L. Seldeen, C.B. McDonald, B.J. Deegan, A. Farooq, Arch. Biochem. Biophys. 473 (2008) 48–60.
[17] E. Gasteiger, C. Hoogland, A. Gattiker, S. Duvaud, M.R. Wilkins, R.D. Appel, A. Bairoch, in: J.M. Walker (Ed.), The Proteomics Protocols Handbook, Humana Press, Totowa, New Jersey, USA, 2005, pp. 571–607.
[18] C.R. Cantor, M.M. Warshaw, H. Shapiro, Biopolymers 9 (1970) 1059–1077.
[19] T. Wiseman, S. Williston, J.F. Brandts, L.N. Lin, Anal. Biochem. 179 (1989) 131–137.
[20] K.P. Murphy, E. Freire, Adv. Protein. Chem. 43 (1992) 313–361.
[21] R.S. Spolar, J.M.T. Record, Science 263 (1994) 777–784.
[22] J. Gomez, V.J. Hilser, D. Xie, E. Freire, Proteins 22 (1995) 404–412.
[23] H. Uedaira, H. Kono, P. Ponraj, K. Kitajima, A. Sarai, Genome Inform. 14 (2003) 510–511.
[24] S.P. Edgcomb, K.P. Murphy, Curr. Opin. Biotechnol. 11 (2000) 62–66.
[25] D. Xie, E. Freire, Proteins 19 (1994) 291–301.
[26] K.P. Murphy, Med. Res. Rev. 19 (1999) 333–339.
[27] E. Freire, Arch. Biochem. Biophys. 303 (1993) 181–184.
[28] R. Fraczkiewicz, W. Braun, J. Comp. Chem. 19 (1998) 319–333.
[29] M.A. Marti-Renom, A.C. Stuart, A. Fiser, R. Sanchez, F. Melo, A. Sali, Annu. Rev. Biophys. Biomol. Struct. 29 (2000) 291–325.
[30] M. Carson, J. Appl. Crystallogr. 24 (1991) 958–961.
[31] H. Kwon, S. Park, S. Lee, D.K. Lee, C.H. Yang, Eur. J. Biochem. 268 (2001) 565–572.
[32] R.P. Ryseck, R. Bravo, Oncogene 6 (1991) 533–542.
[33] Y. Nakabeppu, D. Nathans, Embo. J. 8 (1989) 3833–3841.
[34] F.J. Rauscher 3rd., P.J. Voulalas, B.R. Franza Jr., T. Curran, Genes Dev. 2 (1988) 1687–1699.
[35] C. Berger, I. Jelesarov, H.R. Bosshard, Biochemistry 35 (1996) 14984–14991.
[36] J.H. Ha, R.S. Spolar, M.T. Record Jr., J. Mol. Biol. 209 (1989) 801–816.
[37] J.E. Ladbury, J.G. Wright, J.M. Sturtevant, P.B. Sigler, J. Mol. Biol. 238 (1994) 669–681.
[38] D. Foguel, J.L. Silva, Proc. Natl. Acad. Sci. U. S. A. 91 (1994) 8244–8247.
[39] V. Petri, M. Hsieh, M. Brenowitz, Biochemistry 34 (1995) 9977–9984.
[40] E. Merabet, G.K. Ackers, Biochemistry 34 (1995) 8554–8563.
[41] M. Sieber, R.K. Allemann, Nucleic Acids Res. 28 (2000) 2122–2127.
[42] K. Datta, V.J. LiCata, Nucleic Acids Res. 31 (2003) 5590–5597.
[43] K. Datta, A.J. Wowor, A.J. Richard, V.J. LiCata, Biophys. J. 90 (2006) 1739–1751.
[44] D.A. Leonard, N. Rajaram, T.K. Kerppola, Proc. Natl. Acad. Sci. U. S. A. 94 (1997) 4913–4918.
[45] D.A. Leonard, T.K. Kerppola, Nat. Struct. Biol. 5 (1998) 877–881.
[46] K.P. Murphy, V. Bhakuni, D. Xie, E. Freire, J. Mol. Biol. 227 (1992) 293–306.
[47] P.L. Privalov, S.J. Gill, Adv. Protein Chem. 39 (1988) 191–234.
[48] R.S. Spolar, J.H. Ha, M.T. Record Jr., Proc. Natl. Acad. Sci. U. S. A. 86 (1989) 8382–8385.
[49] P.L. Privalov, G.I. Makhatadze, J. Mol. Biol. 224 (1992) 715–723.
[50] R.S. Spolar, J.R. Livingstone, M.T. Record Jr., Biochemistry 31 (1992) 3947–3955.
[51] M.A. Weiss, T. Ellenberger, C.R. Wobbe, J.P. Lee, S.C. Harrison, K. Struhl, Nature 347 (1990) 575–578.
[52] M.A. Weiss, Biochemistry 29 (1990) 8020–8024.
[53] H.R. Bosshard, E. Durr, T. Hitz, I. Jelesarov, Biochemistry 40 (2001) 3544–3552.
[54] V. Saudek, A. Pastore, M.A. Castiglione Morelli, R. Frank, H. Gausepohl, T. Gibson, F. Weih, P. Roesch, Protein Eng. 4 (1990) 3–10.
[55] K.S. Thompson, C.R. Vinson, E. Freire, Biochemistry 32 (1993) 5491–5496.
[56] J.J. Kohler, A. Schepartz, Biochemistry 40 (2001) 130–142.
[57] E.K. O'Shea, R. Rutkowski, W.F. Stafford 3rd, P.S. Kim, Science 245 (1989) 646–648.
[58] E.K. O'Shea, R. Rutkowski, P.S. Kim, Cell 68 (1992) 699–708.
[59] L.R. Patel, T. Curran, T.K. Kerppola, Proc. Natl. Acad. Sci. U. S. A. 91 (1994) 7360–7364.
[60] D.N. Marti, I. Jelesarov, H.R. Bosshard, Biochemistry 39 (2000) 12804–12818.
[61] D.N. Marti, H.R. Bosshard, Biochemistry 43 (2004) 12436–12447.
[62] R.J. Diebold, N. Rajaram, D.A. Leonard, T.K. Kerppola, Proc. Natl. Acad. Sci. U. S. A. 95 (1998) 7915–7920.
[63] M. John, R. Leppik, S.J. Busch, M. Granger-Schnarr, M. Schnarr, Nucleic Acids Res. 24 (1996) 4487–4494.